Chapter 2
Observing a Vulnerable Carbon Cycle

Michael R. Raupach and Joseph G. Canadell

2.1 Introduction

The carbon cycle and indeed the entire earth system are now inextricably linked with human activities (Global Carbon Project 2003; Steffen et al. 2004; Field and Raupach 2004), so that the 'carbon–climate–human system' constitutes a single, coupled entity in which interacting processes link all of its major components. Linking processes of primary significance include

1. The human drivers of energy consumption and land-use change, through increases in both population and per capita consumption
2. The role of human energy systems as sources of CO_2 and other greenhouse gases (GHGs)
3. Land-use change (deforestation, increases in agricultural and urban land use) and its consequences for both GHG emissions and resource (water, land, ecosystem) condition
4. Climate forcing by CO_2 and other GHGs, following from drivers 1, 2 and 3
5. The changing roles of the ocean and the terrestrial biosphere as sinks and sources of CO_2 and other GHGs, driven by the disequilibrium of the earth system through human activities
6. Impacts of climate change through declines in resource condition and human well-being
7. Attempts by human societies to reduce their impact on the global environment, for example, through reductions in GHG emissions to avoid 'dangerous climate change' (Schellnhuber et al. 2006)

Through the first six of these processes humankind is unintentionally influencing the earth system, while the seventh is an effort to manage global-scale human impacts on the earth system by mitigating their causes.

An integrated global carbon observation system (Ciais et al. 2004) is a contribution to monitoring the first six of the above processes, and bringing about the seventh. These underlying motivations lead to two broad goals for global carbon observations, respectively oriented towards understanding and management. The former goal is to provide increased understanding of the cycles of carbon and

Raupach MR, Canadell JG (2008). Observing a vulnerable carbon cycle. In: The Continental-Scale Greenhouse Gas Balance of Europe (eds. AJ Dolman, R Valentini, A Freibauer). Springer, New York, p. 5-32.

related entities (water, energy, nutrients) in the earth system, contributing to our ability to diagnose trends and to predict future evolution of the carbon–climate system over timescales of decades to centuries. The latter is to provide the global-scale observations of carbon fluxes and GHG emissions needed to manage the carbon cycle, through emissions reduction programmes based on incentive, regulatory or trading mechanisms. Between them, these two goals largely determine the necessary broad attributes of a global carbon observing system. A recent analysis (Raupach et al. 2005) identified seven main attributes for terrestrial carbon observation, which (with slight extension) provide a broad specification of attributes for a complete global carbon observing system. These seven are (1) scientific rigour; (2) global scope and consistency; (3) spatial resolution sufficient to resolve and monitor all important processes, especially carbon fluxes associated with human land use and energy systems; (4) temporal resolution sufficient to monitor variability in fluxes from weather to climate timescales; (5) integrated monitoring of all relevant entities [CO_2, CH_4, CO, volatile organic compounds (VOCs), black carbon, together with fluxes of water, nutrients and other entities relevant in modulating carbon fluxes]; (6) process discrimination (for instance, between anthropogenic and non-anthropogenic fluxes, and between contributions to net fluxes such as assimilation, autotrophic and heterotrophic respiration); and (7) quantification of uncertainty.

Here, we discuss the implications of carbon–climate vulnerabilities for the attributes of an integrated carbon observation system. By 'carbon–climate vulnerability' we mean a positive, disturbance-amplifying feedback between an aspect of the carbon cycle (a pool or flux) and physical climate, including atmosphere, oceans and the hydrological cycle. In particular, carbon–climate vulnerabilities are processes causing global warming through the enhanced greenhouse effect to be larger than it otherwise would be in their absence.

Two ways have been used recently to quantify carbon–climate vulnerability in the above sense. The first is a risk-assessment methodology (Gruber et al. 2004, henceforth G2004) involving heuristic, judgement-based estimates of the releases of carbon to the atmosphere from several terrestrial and oceanic pools under projected changes (to 2100) in temperature, ocean circulation and other physical climate properties. G2004 expressed the results of the assessment as ellipses on a plane with axes defined by the mass of carbon released and a qualitatively judged probability of release (with small releases having high probability and vice versa). This approach is a valuable beginning, but cannot properly quantify carbon–climate feedbacks by estimating the extent to which a carbon release is modified by the extra climate change induced by the release itself.

The second, much more quantitative approach is through the use of fully coupled carbon–climate models. Eleven such models were compared in the recent Coupled Climate–Carbon Cycle Model Intercomparison Project (C^4MIP) (Friedlingstein et al. 2006). The models included full physical climate, ocean carbon biogeochemistry responsive to temperature and atmospheric CO_2 and terrestrial carbon dynamics responsive to light, water, temperature and CO_2. All models were run from 1850 to 2100 under a prescribed emissions scenario (the IPCC SRES[1] A2 scenario; see later

[1] IPCC, Intergovernmental Panel on Climate Change; SRES, Special Report on Emissions Scenarios.

Raupach MR, Canadell JG (2008). Observing a vulnerable carbon cycle. In: The Continental-Scale Greenhouse Gas Balance of Europe (eds. AJ Dolman, R Valentini, A Freibauer). Springer, New York, p. 5-32.

for details). The results showed that coupling of the carbon cycle to climate through temperature-dependent processes led to increased atmospheric CO_2 in 2100 of 20–200 ppm (augmenting a CO_2 concentration of around 700 ppm, depending on the model) and an increase in predicted global temperature of 0.2–2 °C (augmenting an enhanced-greenhouse-induced warming of around 4 °C, likewise depending on the model). There were substantial differences among the ten models, stemming both from carbon cycle parameterisations (for instance, the temperature response of terrestrial heterotrophic respiration) and from the behaviour of modelled physical climate (for instance, the tendency of some of the models to dry out the Amazon as the model climate warms). As a means of studying carbon–climate vulnerabilities, fully coupled carbon–climate models are comprehensive, but they are laborious and difficult to parameterise because of model complexity. The extensive C⁴MIP runs to date have focused on only a few of the potentially important feedback processes.

In this chapter, we analyse carbon–climate vulnerability and its implications for carbon cycle observations. The plan of the chapter (following this brief introductory section) is that Sect. 2.2 surveys the major feedbacks in the carbon–climate–human system at a general level, including forcing by and feedbacks on human actions. Section 2.3 focuses on carbon–climate feedbacks involving terrestrial processes, drawing from C⁴MIP results and other sources. Attention is given to both CO_2 and CH_4. Section 2.4 proposes a perturbation-based approach using simple models for analysing carbon–climate vulnerabilities and illustrates the approach with a semi-quantitative evaluation of the response of permafrost carbon pools to global change. Finally, Sect. 2.5 discusses the implications of carbon vulnerability for integrated carbon observation.

2.2 Feedbacks and Vulnerabilities in the Carbon–Climate–Human System

The trajectories of climate and the carbon cycle are coupled by atmospheric composition. Of the linking groups of processes mentioned in Introduction, four are of central importance for feedbacks and vulnerabilities in the contemporary carbon–climate–human system. The first is enhanced radiative forcing by GHGs, CO_2 and CH_4 being the largest contributors. The other three correspond to the three major groups of fluxes in the atmospheric CO_2 and CH_4 budgets: emissions from human activities, ocean–atmosphere exchanges and land–atmosphere exchanges. Section 2.2.1 focuses on land–atmosphere exchanges in more detail, but before doing so, we examine all four groups of processes in general terms.

2.2.1 Radiative Forcing

The carbon cycle accounts for some, but not all, of the processes involved in the radiative forcing of climate. Total radiative forcing can be considered as the sum of

Raupach MR, Canadell JG (2008). Observing a vulnerable carbon cycle. In: The Continental-Scale Greenhouse Gas Balance of Europe (eds. AJ Dolman, R Valentini, A Freibauer). Springer, New York, p. 5-32.

three contributions: (1) from CO_2, (2) from non-CO_2 GHGs (mainly CH_4, halocarbons, N_2O, ozone) and (3) from non-gaseous mechanisms (mainly aerosols, albedo changes, solar variations). The first two are relatively well known (IPCC 2007): the current (2001–2005) radiative forcing from CO_2 is $+1.66 \pm 0.17\,W\,m^{-2}$, and the forcing from non-CO_2 GHGs is about $+1.3\,W\,m^{-2}$ (+0.48 from CH_4, +0.34 from halocarbons, +0.16 from N_2O and +0.30 from ozone). The third contribution, from aerosols, albedo changes and solar variations, is highly uncertain but is considered to be negative, current estimates being around $-1.3 \pm 1\,W\,m^{-2}$ (IPCC 2007). The current net radiative forcing ($+1.6\,W\,m^{-2}$, range +0.6 to +2.4) drives global warming (at about 0.016 °C y^{-1}over the period 1980–2005). Thus, current net radiative forcing is approximately equal to the radiative forcing from CO_2 alone, with other contributions approximately cancelling. This does not imply that *future* forcing will behave this way, because all three contributions to radiative forcing are dependent on emissions scenarios and also on future climate through climate feedbacks, so the three contributions will evolve differently under these influences. In summary, a carbon budget and a radiative forcing budget are different entities, but they share a large common term associated with rising atmospheric CO_2.

2.2.2 Emissions from Human Activities

The global balance of atmospheric CO_2, shown in Fig. 2.1, demonstrates that human activities are the overwhelmingly dominant contribution to the current disequilibrium of the global carbon cycle. Fossil-fuel emissions were about 7.2 ± 0.3 Pg C y^{-1} for the period 2000–2005, and increased at over 3% y^{-1} for 2000–2005 compared with 1% y^{-1} for 1990–1999 (Canadell et al. 2007a; Raupach et al. 2007). Emissions from land clearing have changed more slowly, averaging about 1.5 ± 0.5 Pg C y^{-1} (Canadell et al. 2007a).

The atmospheric CH_4 balance involves ten major source terms and three sink terms, and is discussed in more detail later. Of the current total source, about 2/3 is anthropogenic.

The four main groups of IPCC SRES scenarios (Nakicenovic et al. 2000) all involve major increases in CO_2 emissions over the period to 2100 (Table 2.1), ranging from 12 to 17 Pg C y^{-1} in 2050 and from 7 to 30 Pg C y^{-1} in 2100. Methane emissions are also projected to increase in most scenarios. From the present standpoint of vulnerability analysis, the important question is: are these emissions scenarios significantly dependent on climate itself, so that different emissions scenarios would result from different climate change scenarios? While climate is just one among the many economic, social and environmental factors influencing the scenarios, there are potential mechanisms for feedbacks on emissions scenarios from climate change. Examples include increased energy use to buffer against adverse effects of climate change (e.g. air conditioning), increased energy use to augment resources threatened by climate change (e.g. desalination to supplement water supplies) and increased military energy use brought on by climate-induced geopolitical instability.

Raupach MR, Canadell JG (2008). Observing a vulnerable carbon cycle. In: The Continental-Scale Greenhouse Gas Balance of Europe (eds. AJ Dolman, R Valentini, A Freibauer). Springer, New York, p. 5-32.

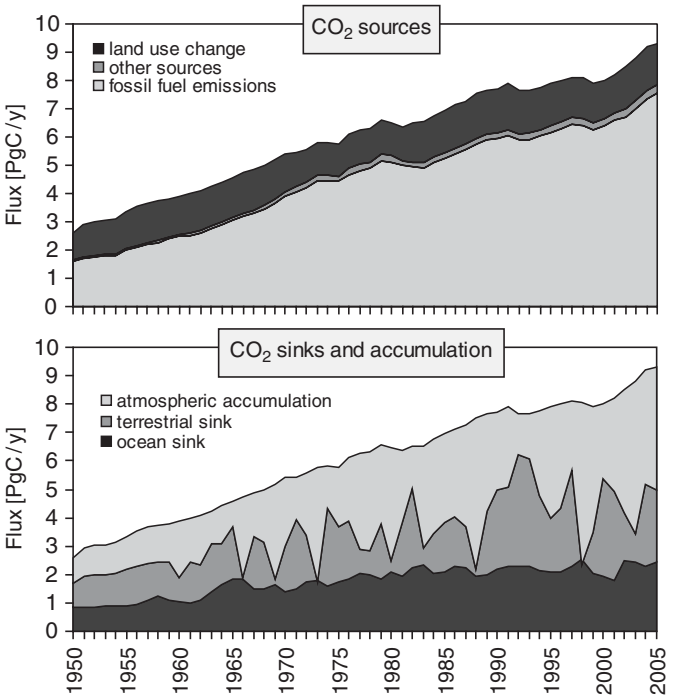

Fig. 2.1 The global carbon budget for the period 1950–2005, showing terms in the CO_2 mass balance: [atmospheric CO_2 accumulation] = [emission flux from fossil fuels] + [other industrial emissions] + [emissions from land-use change] − [flux to terrestrial sink] − [flux to ocean sink]. Data sources as in Canadell et al. (2007a), with atmospheric CO_2 change from ice core data (Law Dome, Antarctica; Etheridge et al. 1998b) before 1959 and direct measurements (Keeling and Whorf 2005) after 1959. Net terrestrial uptake is inferred by difference (total emissions less ocean uptake).

Table 2.1 Indicative fossil-fuel emissions of CO_2 under four major IPCC SRES emissions scenarios (Nakicenovic et al. 2000)

Scenario	Global-local orientation	Economic-environmental orientation	Fossil-fuel emission (Pg C y^{-1}) in 2050	Fossil-fuel emission (Pg C y^{-1}) in 2100
A1B	Global	Economic	17	15
A2	Regional	Economic	15	30
B1	Global	Environmental	11	15
B2	Regional	Environmental	12	7

There are three variants of the A1 (globalised, economically oriented) scenario: A1B (balanced), A1T (technologically innovative) and A1FI (fossil-fuel intensive), leading to very different emissions trajectories. Only the A1B scenario is used here

2.2.3 Ocean–Atmosphere Exchanges

The ocean is a major CO_2 sink, currently absorbing about 25% of fossil-fuel emissions (Fig. 2.1). This will continue over the next century according to C^4MIP carbon–

Raupach MR, Canadell JG (2008). Observing a vulnerable carbon cycle. In: The Continental-Scale Greenhouse Gas Balance of Europe (eds. AJ Dolman, R Valentini, A Freibauer). Springer, New York, p. 5-32.

climate models (Friedlingstein et al. 2006). There are several timescales for ocean–atmosphere exchanges related to different ocean carbon pools, but even the shortest is long enough for ocean uptake of CO_2 to be fairly smooth from year to year (Fig. 2.1). Several reviews (Jacobson et al. 2000; Steffen et al. 2004; Le Quere and Metzl 2004; Greenblatt and Sarmiento 2004) describe the processes involved, which include (1) *air–sea exchange* of CO_2, driven by the difference in CO_2 partial pressure (pCO_2) between atmosphere and ocean surface waters; (2) *buffering* between dissolved CO_2 and DIC (total inorganic carbon including CO_2, H_2CO_3, HCO_3^- and CO_3^{2-}), which means that only about 10% of the carbon crossing the air–sea interface contributes to aqueous pCO_2, with the rest appearing as other forms of DIC; (3) *the ocean circulation pump*, by which ocean circulations export carbon from surface to deep ocean waters and (4) *biological pumps*, by which soft-tissue and carbonate detritus from ocean biota in the surface layer export carbon to deep waters as they sink.

All of these processes are subject to climate feedbacks. G2004, in their risk-assessment-based analysis of carbon cycle vulnerabilities, identified six feedbacks. First, chemistry leads to a positive feedback because ocean pH falls as CO_2 is taken up, thereby altering the CO_2/DIC partition and reducing uptake. Second, temperature increases lead to a similar positive feedback through the CO_2/DIC partition. Third, changes in deep ocean circulation (mainly through increasing vertical stratification) increase ocean equilibration times, inducing a positive feedback through reduced uptake over timescales of 10–100 years since the mixing timescale becomes longer. Fourth, ocean circulation changes alter the equilibrium carbon distribution itself (in addition to changing the equilibration timescale), which when coupled with the biological pump leads to a negative feedback because upward transport of DIC from deep to surface waters is reduced but the downward biological pump is not. Fifth, the biological pump is subject to large influence by climate change, but uncertainties are so high that it is not yet possible to identify whether these influences add up to an overall positive or a negative feedback. Sixth, there is the possibility of release from the vast stores of methane hydrates in sediments under continental shelves (and in permafrost). Such a release would constitute a massive positive (heating) feedback on the climate system, but is rated by G2004 as a high-risk, low-probability scenario.

2.2.4 Land–Atmosphere Exchanges

Like the oceans, the terrestrial biosphere currently takes up about 25% of fossil-fuel emissions of CO_2, but unlike the ocean sink, the terrestrial CO_2 sink varies enormously from year to year (Fig. 2.1). Similarly, on longer (100 year) timescales, C^{4}MIP results suggest higher variability for the terrestrial than the ocean CO_2 sink, both in time and between individual models in C^{4}MIP. Land–atmosphere exchanges are also critical in the CH_4 budget. These issues are explored in more detail in Sect. 2.3.

Raupach MR, Canadell JG (2008). Observing a vulnerable carbon cycle. In: The Continental-Scale Greenhouse Gas Balance of Europe (eds. AJ Dolman, R Valentini, A Freibauer). Springer, New York, p. 5-32.

2.3 Vulnerabilities in Terrestrial Carbon Pools and Fluxes

The terrestrial carbon balance equates the net change in terrestrial-biospheric carbon to the sum of carbon fluxes into the terrestrial carbon pool. These fluxes include land–air gaseous exchanges, waterborne and airborne particulate transport, and product removal by humans. The focus here is on the first, which is the most significant for the global carbon budget (though the others can be important particularly for regional carbon budgets). Gaseous carbon exchange between terrestrial systems and the atmosphere occurs through fluxes of CO_2 and several other species including CH_4, VOCs and CO. The CO_2 exchange dominates the mass flux, but exchanges of other species have significant effects on radiative forcing. Here, we summarise the main processes leading to vulnerabilities in land–air exchanges of carbon as CO_2 and CH_4, since these two entities are the most important from both mass-flux and radiative forcing standpoints.

2.3.1 Vulnerabilities Associated with CO_2 Exchanges

Table 2.2 summarises the main processes affecting the net land-atmosphere flux of CO_2 in terrestrial systems. The table identifies three classes of driver for changes in

Table 2.2 Processes contributing to net land–atmosphere exchange of CO_2

	Process	Driver	Sign of land-to-air flux (+,−) =(source, sink)
a1	CO_2 fertilisation	*a*	−
a2	Nutrient constraints on CO_2 fertilisation	*a*	+
a3	Fertilisation by nitrogen deposition	*a*	−
a4	Effects of pollution (e.g. acid rain, ozone, etc.)	*a*	+
b1	Response of respiration to warming and moisture	*b*	+ (warming), ± (moisture)
b2	Response of NPP to warming and moisture	*b*	− (warming), ± (moisture)
b3	Radiation effects (e.g. direct/diffuse partition)	*b*	−
b4	Biome shifts	*b*	±
b5	Permafrost thawing	*b*	+
b6	Changes in wildfire regime	*b*	+ (rapid), − (slow)
b7	Changes in herbivore (e.g. insect) ecology	*b*, *c*	+
c1	Changes in managed fire regime	*c*	+ (rapid), − (slow)
c2	Managed reforestation and afforestation	*c*	−
c3	Unmanaged forest regrowth (after cropland abandonment)	*c*	−
c4	Woody encroachment/woody thickening	*c*	−
c5	Deforestation and land clearing (e.g. forest to savannah)	*c*	+
c6	Peatland and wetland drainage	*c*	+
c7	Agricultural practices	*c*	±

Drivers are (*a*, shaded grey) changes in atmospheric composition and chemistry; (*b*, unshaded) physical climate changes; (*c*, shaded grey) changes in land use and land management. The sign of the land-to-air CO_2 flux is the same as the sign of the climate warming feedback (a positive land-to-air flux increases the CO_2 radiative forcing)
NPP net primary production

Raupach MR, Canadell JG (2008). Observing a vulnerable carbon cycle. In: The Continental-Scale Greenhouse Gas Balance of Europe (eds. AJ Dolman, R Valentini, A Freibauer). Springer, New York, p. 5-32.

these processes: (*a*) changes in atmospheric composition (CO_2 fertilisation, nutrient effects, pollution effects); (*b*) changes in physical climate (temperature, precipitation, light) and (*c*) changes in land use and land management. Table 2.2 also identifies whether the process is a source or a sink, an attribute that has no simple correlation with the class of driver. All processes driven by changes in atmospheric composition (*a*) and physical climate (*b*) are directly involved in carbon–climate feedbacks. An additional dimension to terrestrial carbon vulnerability arises through processes driven by changes in land use and land management (*c*), which provide direct couplings between the terrestrial carbon cycle and human actions in the carbon–climate–human system.

Most of the processes listed in Table 2.1 are vulnerable to major changes over the next century, and many have already changed significantly over the last century. The most important feedbacks and vulnerabilities associated with these processes can be summarised as follows, drawing from a recent review (Canadell et al. 2007b; henceforth C2007). (Note that not all processes listed in Table 2.2 are discussed in the following.)

2.3.1.1 CO_2 Fertilisation and Its Limitation by Water and Nutrient Constraints *(a1, a2)*

It is expected on physiological grounds that plants respond to rising atmospheric CO_2 with increased assimilation, leading to increased biomass. The response saturates at around 1,000 ppm according to models and laboratory experiments (Farquhar et al. 1980; Farquhar and Sharkey 1982). This CO_2 fertilisation process is now incorporated in most terrestrial–biosphere and dynamic-vegetation models (Cramer et al. 2001). However, field results from free air CO_2 enrichment (FACE) and other elevated CO_2 studies have been variable (Oren et al. 2001; Nowak et al. 2004; Norby et al. 2005). Some actively growing vegetation types (such as temperate, well-watered young forests) show responses in net primary production (NPP) of up to 25% (Norby et al. 2005), while other, more stressed vegetation types show much lower responses (Nowak et al. 2004). Field observations also indicate a saturation of response to CO_2 fertilisation at 500–600 ppm, much lower than expected on physiological grounds. These results indicate that the full possible physiological response to CO_2 fertilisation is not manifested in most field environments because of constraints from factors other than CO_2, especially nitrogen limitations (Luo et al. 2004). There is also an interaction between water limitation and CO_2 fertilisation through the beneficial (to terrestrial carbon storage) effect of increasing CO_2 on water-use efficiency because of decreased stomatal conductance. This is most pronounced in dry ecosystems (Field et al. 1996; Owensby et al. 1997; Pataki et al. 2000).

2.3.1.2 Fertilisation by Nitrogen Deposition *(a3)*

Early studies (Townsend et al. 1996; Holland et al. 1997) suggested significant enhancement of the terrestrial CO_2 sink by N deposition, especially in mid-latitude

Raupach MR, Canadell JG (2008). Observing a vulnerable carbon cycle. In: The Continental-Scale Greenhouse Gas Balance of Europe (eds. AJ Dolman, R Valentini, A Freibauer). Springer, New York, p. 5-32.

Northern Hemisphere forests where N limitation is common and deposition rates are high. Later work (Nadelhoffer et al. 1999) has suggested a lower contribution of about 0.25 Pg C y^{-1} to the current net terrestrial sink of 2–3 Pg C y^{-1}. C2007 concluded that it is unlikely that N deposition will create major new carbon sinks over the next century.

2.3.1.3 Response of Respiration to Warming and Moisture *(b1)*

Warming increases heterotrophic respiration of soil carbon (R), thus decreasing Net Ecosystem Exchange (NEE = NPP − R). Soil moisture is comparably important. Most models incorporate a strong temperature response of soil respiration, quantified by $Q_{10} = R(T + 10\,°\mathrm{K})/R(T)$, which is a dominant contributor to the source side of the terrestrial carbon balance and is a major reason for predictions that the current terrestrial sink will saturate or reverse in the future. Most of the 11 C^4MIP models used $Q_{10} = 2$ (Friedlingstein et al. 2006). However, as usual, experimental evidence is less clear-cut than modelling assumptions. The review of C2007 is summarised here in three stages: first, many laboratory and some field studies support high Q_{10} values of 2 or more for soil respiration, and show that Q_{10} decreases with increasing temperature (Lloyd and Taylor 1994). Second, other field studies (Giardina and Ryan 2000; Valentini et al. 2000; Jarvis and Linder 2000; Luo et al. 2001) have suggested that Q_{10} declines after some time as labile soil carbon is respired, leaving more recalcitrant soil carbon for which turnover is slower and less sensitive to temperature. Third, recent studies (Knorr et al. 2005; Fang et al. 2005) have resolved the apparent paradox by analysing the data in terms of separate fast and slow carbon pools (in contrast with earlier studies which analysed all soil carbon in one pool). These newer studies find different temperature dependences in R for fast and slow soil carbon pools, with faster pools having more temperature sensitivity.

2.3.1.4 Response of NPP to Warming and Moisture *(b2)*

Global terrestrial NPP has increased by 6% (3.4 Pg C y^{-1}) over the two decades from 1981 to 2000, largely because of extension of the growing season in high–northern-latitude ecosystems because of global warming (Nemani et al. 2003). This is associated with an increase in the terrestrial CO_2 sink (excluding land-use change) from around 0.3 Pg C y^{-1} in the 1980s to 2–3 Pg C y^{-1} in the 1990s (IPCC 2001; Sabine et al. 2004). Most (though not all) C^4MIP simulations predict a further increase in the terrestrial CO_2 sink through the twenty-first century, driven largely by CO_2 fertilisation (Friedlingstein et al. 2006). This would provide a negative feedback on further climate change. However, new observations of a reduced CO_2 sink due to increased climate variability are challenging the hypothesis of an increasing terrestrial CO_2 sink in the twenty-first century. An analysis of Northern Hemisphere terrestrial carbon fluxes (Angert et al. 2005) shows that since 1994,

Raupach MR, Canadell JG (2008). Observing a vulnerable carbon cycle. In: The Continental-Scale Greenhouse Gas Balance of Europe (eds. AJ Dolman, R Valentini, A Freibauer). Springer, New York, p. 5-32.

accelerated carbon uptake in early spring was cancelled by decreased uptake during summer, most likely due to hotter and drier summers in middle and high latitudes. The heatwave in 2003 alone reduced the gross primary productivity of European ecosystems by 30%, resulting in a net atmospheric CO_2 source of 0.5 Pg C y^{-1} or 4 years of carbon accumulation in these systems (Ciais et al. 2005).

2.3.1.5 Permafrost Thawing *(b5)*

The carbon store in frozen soils in the Northern Hemisphere has been estimated as over 400 Pg C, of which around 54% is in Eurasia, largely in Russia, and 46% in North America, largely in Canada (Tarnocai 1999). A recent estimate is substantially higher at around 900 Pg C (Zimov et al. 2006). Widespread observations already exist of permafrost thawing leading to the development of thermokarst and lake expansion, followed by lake drainage as permafrost further degrades (Camill 2005; Smith et al. 2005; Jorgenson et al. 2006). Preliminary estimates suggest that permafrost area could shrink by up to 25% with a mean global warming of 2 °C (Anisimov et al. 1999). Melting permafrost will increase both CO_2 and CH_4 emissions from frozen soils. It is estimated for the Canadian permafrost alone that up to 48 Pg C could be vulnerable to release under a 4 °C warming scenario (Tarnocai 1999). G2004 suggested that up to 5 Pg C could be released from melting permafrost over the next 20 years and up to 100 Pg C in the next 100 years, assuming a warming of 2 °C by 2100 and that this warming releases 25% of the carbon locked in frozen soils (following projected area reductions).

2.3.1.6 Fire *(b6, c1)*

The annual carbon flux to the atmosphere from savannah and forest fires (excluding biomass burning for fuel and land clearing) is estimated to be in the range of 1.7–4.1 Pg C y^{-1} (Mack et al. 1996), mostly as CO_2. A recent estimate (van der Werf et al. 2006) gives a fire emission of 2.5 Pg C y^{-1} 1997–2004. In high-intensity fire years such as during El Niño-Southern Oscillation (ENSO) events, emission from fires can be responsible for as much as 66% of the atmospheric CO_2 growth anomaly (van der Werf et al. 2003). In the long term or over large spatial regions, terrestrial carbon losses from fires may be compensated by the gains during vegetation regrowth. However, a terrestrial carbon imbalance is created during the transition from one disturbance regime to another: this leads to a CO_2 sink (or source) when the disturbance frequency is reduced (or increased). Furthermore, trends in fire disturbance frequency are not spatially uniform. For instance, fire exclusion during the twentieth century in many countries has resulted in an increase of biomass in forests and woodlands (Luger and Moll 1993; Houghton et al. 2000; Mouillot and Field 2005), and the potential exists for further accumulation especially in temperate and subtropical regions. By contrast, increases in annual burned area over the last two decades in boreal North America and some parts of Europe are shifting a

Raupach MR, Canadell JG (2008). Observing a vulnerable carbon cycle. In: The Continental-Scale Greenhouse Gas Balance of Europe (eds. AJ Dolman, R Valentini, A Freibauer). Springer, New York, p. 5-32.

long-term trend of terrestrial carbon accumulation into one of release to the atmosphere (Kurz and Apps 1999).

2.3.1.7 Managed and Unmanaged Forest Growth *(c2, c3, c4)*

Directly and indirectly human-induced forest regrowth (through cropland abandonment, vegetation thickening, afforestation and reforestation) accounts for a major contribution to the terrestrial carbon sink of 2–3 Pg C y^{-1} through the 1990s. Several processes are involved, all related to land use and land management. First, forest regrowth on abandoned agricultural land has been identified as one of the most significant mechanisms to explain the net CO_2 sink in the Northern Hemisphere, both in the USA (Houghton and Hackler 2000) and in Europe (Janssens et al. 2005). Crop abandonment results in the expansion of relatively young forests with fast growth rates, and therefore with high CO_2 sink capacity. Second, woody thickening and encroachment in semi-arid regions and savannahs, largely due to fire suppression policies and pasture management, accounts for 22–40% of the US terrestrial carbon sink (Pacala et al. 2001) and is a significant component of the sink in Australia (Gifford and Howden 2001; Burrows et al. 2002). However, these estimates have very large uncertainties. Third, managed afforestation and reforestation has a significant potential as a terrestrial CO_2 sink over the twenty-first century, though currently only China has seen a substantial increased terrestrial carbon storage (0.45 Pg C) by this mechanism, through large reforestation efforts over recent decades (Fang et al. 2001).

2.3.1.8 Deforestation and Land Clearing *(c5)*

Deforestation and land clearing, mainly to establish croplands, has released a total of 182–199 Pg C to the atmosphere over the period from 1800 to 2000 (DeFries et al. 1999) and is responsible for 33% of the increase in atmospheric CO_2 concentration observed over that period (Houghton 1998). Estimates of emissions from deforestation for the decades of the 1980s and 1990s range from 0.8 to 2.2 Pg C y^{-1} (DeFries et al. 2002; Houghton 2003; Achard et al. 2004) and are expected to continue being significant over the next decades to century.

2.3.1.9 Peatland and Wetland Drainage *(c6)*

Peatlands and wetlands in high, temperate and tropical latitudes contain a carbon store of over 450 Pg C, as soil organic matter. This carbon is largely isolated from decomposition by waterlogged environments and/or low temperatures, but is vulnerable to release to the atmosphere when water tables fall (through land-use change or precipitation change) or temperatures rise. When such carbon releases occur, a complex balance exists between CO_2 emissions (in oxidising conditions

Raupach MR, Canadell JG (2008). Observing a vulnerable carbon cycle. In: The Continental-Scale Greenhouse Gas Balance of Europe (eds. AJ Dolman, R Valentini, A Freibauer). Springer, New York, p. 5-32.

associated with falling water tables) and CH_4 emissions (in anoxic conditions associated with high water tables). A Siberian wetland illustrates this complexity (Friborg et al. 2003): despite being a net carbon sink, the wetland was a source of positive radiative forcing because of its emissions of CH_4 (which has a warming potential 21 times larger than that of CO_2 over 100 years). The case of tropical peatlands is particularly important because of high vulnerabilities driven by both land use and climate factors. The carbon store in tropical peatlands is about 70 Pg C, with deposits as deep as 20 m (Page et al. 2002) much of it in the south-east Asian archipelago (Indonesia, Malaysia, Papua New Guinea, Thailand, Philippines). These peatlands have been a net CO_2 sink since the late Pleistocene (Page et al. 2004). However, over the last decade, a combination of intense draining for agriculture and increasing climate variability (in the form of more intense El Niño-drought events) has resulted in a significant CO_2 source with discernible effects on atmospheric CO_2 growth. During El Niño 1997–1998 events in Indonesia, burning of peat and vegetation resulted in an estimated loss of carbon between 0.81 and 2.57 Pg C in 1997, equivalent to 13–40% of the mean annual global carbon emissions from fossil fuels (Page et al. 2002) and a 60% contribution to the atmospheric CO_2 growth anomaly due to fire activity (van der Werf et al. 2004).

2.3.2 *Vulnerabilities Associated with CH_4 Exchanges*

The atmospheric methane concentration is currently about 1,750 ppb (mole fraction), having risen from around 600 ppb in the pre-industrial era (Fig. 2.2). The growth rate of atmospheric CH_4 has declined over recent years to the point where it is now nearly zero (Allan et al. 2005; Bousquet et al. 2006). The CH_4 growth rate is controlled by an atmospheric methane budget which includes a number of different sources and sink terms, and can be written for the present purpose as:

$$r_{CH_4}\frac{d\left[CH_4\right]}{dt} = \underbrace{\begin{pmatrix} F_{Wetlands} + F_{Termites} + F_{Ocean} + F_{Geol} \\ F_{Fuels} + F_{Landfills} + F_{Ruminants} + F_{Rice} + F_{Fire} + F_{Other} \end{pmatrix}}_{Sources} - \underbrace{(F_{Trop\,OH} + F_{Soils} + F_{Stat})}_{Sinks} \qquad (2.1)$$

$$\frac{d\left[CH_4\right]}{dt} \approx r_{CH_4}^{-1} F_{Sources} - k_{CH_4}\left[CH_4\right]$$

where r_{CH4} is the mass of atmospheric methane per unit concentration and k_{CH4} is an overall decay rate. The sources can be categorised as non-anthropogenic and anthropogenic (respectively grouped on the first and second lines of the 'source' collection of fluxes above). Non-anthropogenic sources arise from wetlands, termites, ocean sources (including methane hydrates) and geological processes (geothermal and volcanic). Anthropogenic CH_4 sources, which are amenable to mitigation, result from burning and leakage of fossil fuels (natural gas, petroleum, coal), landfills, ruminant livestock, rice paddies and biomass burning associated with land clearing. The largest sink is from tropospheric OH oxidation, with smaller sinks

Raupach MR, Canadell JG (2008). Observing a vulnerable carbon cycle. In: The Continental-Scale Greenhouse Gas Balance of Europe (eds. AJ Dolman, R Valentini, A Freibauer). Springer, New York, p. 5-32.

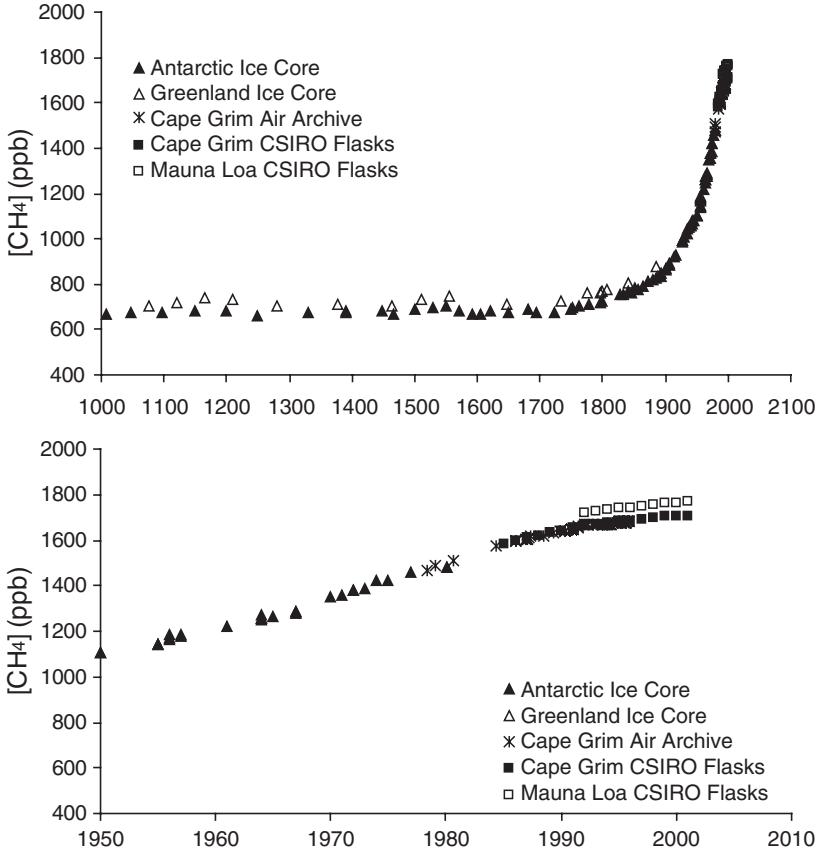

Fig. 2.2 Atmospheric CH_4 concentrations from ice core data from Law Dome, Antarctica, and Summit, Greenland (Etheridge et al. 1998a); the Cape Grim Air archive (Etheridge et al. 1998a) and flask measurements at Cape Grim, Tasmania, and Mauna Loa, Hawaii (CSIRO flask network, archived at http://cdiac.ornl.gov/trends/atm_meth/csiro/csiro_gaslabch4.html). Upper and lower panels show data on 1,000-year and 50-year time axes, respectively.

arising from soils, oceanic and stratospheric oxidation. The sinks can be parameterised as a first-order decay with a turnover time ($1/k_{CH4}$) of about 10 years. Provided k_{CH4} is steady, this implies that

$$[\mathrm{CH_4}](t) \approx \int_0^\infty F_{\mathrm{Sources}}(t-s)\exp(-k_{\mathrm{CH_4}}s)\,\mathrm{d}s \tag{2.2}$$

so the CH_4 concentration is a lagged moving time average of the sources with an exponential weighting factor in time.

Figure 2.3 shows estimates from several studies of the CH_4 source and sink terms in Eq. (2.1). Approximately 2/3 of global emissions are currently from anthropogenic sources. Estimates of the sources are quite scattered, with each of the

Raupach MR, Canadell JG (2008). Observing a vulnerable carbon cycle. In: The Continental-Scale Greenhouse Gas Balance of Europe (eds. AJ Dolman, R Valentini, A Freibauer). Springer, New York, p. 5-32.

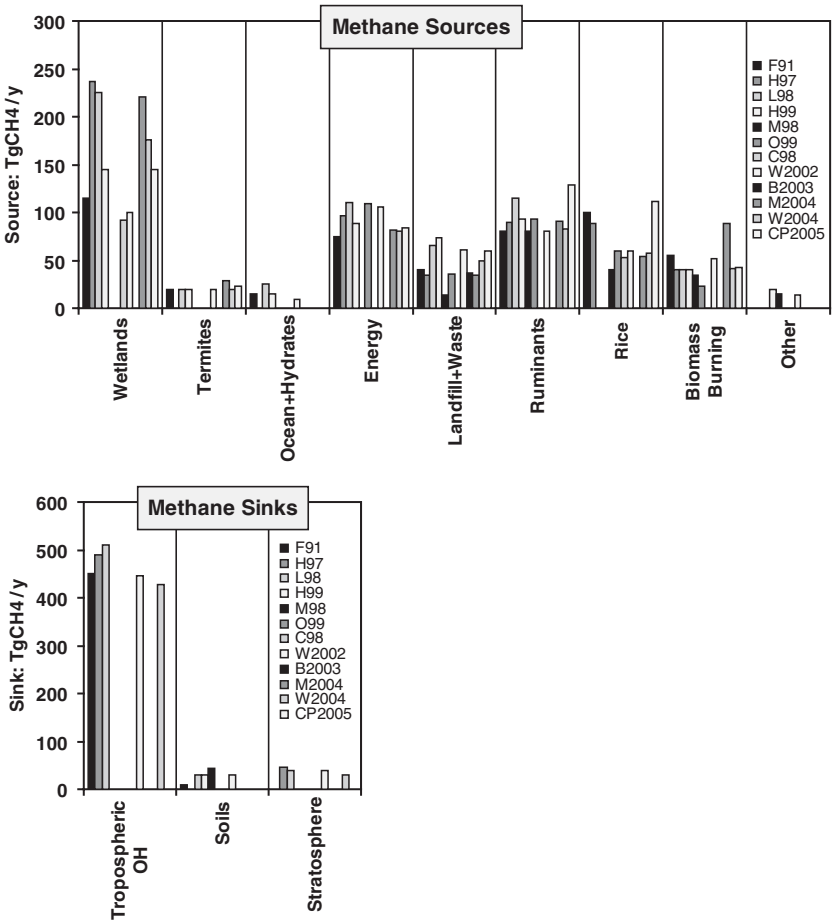

Fig. 2.3 Estimates of sources (upper panel) and sinks (lower panel) in the global atmospheric methane budget. Note different scales. References: Fung et al. 1991 (F91); Hein, Crutzen and Heimann 1997 (H97); Lelieveld, Crutzen and Dentener 1998 (L98); Houweling et al. 1999 (H99); Mosier et al. 1998 (M98); Olivier et al. 1999 (O99); Cao, Gregson and Marshall 1998 (C98); Wuebbles and Hayhoe 2002 (W2002); Bogner and Matthews 2003 (B2003); Mikaloff Fletcher et al. 2004a; Mikaloff Fletcher et al. 2004b (M2004); Wang et al. 2004 (W2004); Chen and Prinn 2005 (CP2005). A 4-level greyscale is used to distinguish studies, cycling 3 times through the 12 available studies.

major anthropogenic sources (fossil fuels, landfills, ruminants, rice, biomass burning) contributing significantly (in the order of 50–100 Tg CH_4 y^{-1}) to the total current source of about 500 Tg CH_4 y^{-1}. The recent reduction in the growth rate of atmospheric CH_4 to near zero (Fig. 2.2) results from decreased fossil-fuel-related anthropogenic emissions through the 1990s, and decreased emissions since 1999 from drying wetlands in temperate and tropical Asia and tropical South America, combined with a return to rising anthropogenic emissions (Bousquet et al. 2006).

Raupach MR, Canadell JG (2008). Observing a vulnerable carbon cycle. In: The Continental-Scale Greenhouse Gas Balance of Europe (eds. AJ Dolman, R Valentini, A Freibauer). Springer, New York, p. 5-32.

Despite the recent slow down in CH_4 growth rate, most SRES scenarios predict that atmospheric CH_4 emissions will increase by a factor of typically 1.5–2 in the century to 2100 (with much scatter among scenarios). These predicted increased emissions result from all the anthropogenic sources listed above. In addition, future methane vulnerabilities can arise from mechanisms which cause either non-anthropogenic or anthropogenic CH_4 sources to increase in response to climate change. Increased temperatures and atmospheric CO_2 will increase CH_4 production from wetlands and rice paddies as more substrate is made available. More importantly, however, is the control that the water table exercises on CH_4 wetland sources. Overall increase in precipitation in a warmer climate will enhance this source by raising water tables, but regional drying trends will result in decreased CH_4 production and a simultaneous increase in CO_2 emissions (Christiansen et al. 2003; Cao et al. 1998). This issue is similar to that for peatland and wetland drainage, discussed above for CO_2 emissions.

2.4 Semi-Quantitative Evaluation of Carbon–Climate Vulnerabilities

Evaluation of future carbon–climate vulnerabilities is not easy. The first requirement is a quantitative definition, here constructed as follows: we imagine a model of the carbon–climate system which includes a coupling or feedback process P between carbon and climate (such as any of the processes in Table 2.2). Starting from a given initial state of the system, the model can be integrated forward in time to produce estimates of the state $\mathbf{x}(t)$ of the system at any future time t. This integration can be carried out for an 'uncoupled' version of the model in which the process P is omitted from the model equations, and for a 'coupled' version in which P is included. For a variable y in the carbon–climate system such as atmospheric CO_2 or temperature [or in general any function of the state vector $\mathbf{x}(t)$], the vulnerability of y to P at time t can be defined as

$$\delta y(t) = y_C(t) - y_U(t) \tag{2.3}$$

where $y_C(t)$ and $y_U(t)$ are respectively the values of $y(t)$ from the coupled and uncoupled versions of the model. Under this quantitative definition, the vulnerability is specific to a variable y (such as a carbon pool), a process P and a time t. It is a model-based, 'what-if' measure of the significance of process P. [This definition is not the same as the sensitivities used in C⁴MIP analyses, which are linearised relationships between $\delta y_1(t)$ and $\delta y_2(t)$ for different model variables y_1 and y_2, for example, the sensitivity of terrestrial or ocean carbon uptake to CO_2 or temperature.]

In Introduction to this chapter, we have already reviewed the two main ways that have been used recently to explore carbon–climate vulnerability: the judgement-based, risk-assessment approach of G2004, and fully coupled carbon–climate models as in the C\⁴MIP experiments (Friedlingstein et al. 2006). These approaches have

Raupach MR, Canadell JG (2008). Observing a vulnerable carbon cycle. In: The Continental-Scale Greenhouse Gas Balance of Europe (eds. AJ Dolman, R Valentini, A Freibauer). Springer, New York, p. 5-32.

complementary strengths: the risk-assessment approach is subjective, exploratory and largely non-quantitative. The fully coupled model approach is quantitative and rigorous (within the parameterisation choices in particular models) but is subject to the usual difficulties of complex, numerically intensive models: (1) model parameterisations (functional relationships between fluxes and model state variables) are scale dependent (Raupach et al. 2005) and hence not unique, so that their choice involves an element of subjective judgement; (2) the settings of parameter values (numbers in the functional relationships) are usually underdetermined by available information; (3) complex models are usually numerically intensive and expensive to integrate over long times (particularly in ensemble mode to assess the properties of model solutions which are chaotic attractors), which places a practical restriction on the range of processes (P) which can be assessed.

For these reasons, it is appropriate to explore an intermediate pathway for assessing carbon–climate vulnerability, based on very simple but still quantitative models which preserve the essential carbon–climate feedbacks leading to possible vulnerabilities. Criteria for a simple model to be used in this way are that the model broadly reproduces (1) observed features of past changes in the carbon–climate system over the last 200 years; (2) the future predictions of more complex models, such as carbon–climate trajectories under the four main classes of IPCC scenario (Table 2.1); (3) the model must include defensible (though necessarily simple) parameterisations of processes (P) to be assessed for vulnerability which are not currently included in more complex models. The basic assumption is that although a simple model cannot provide a stand-alone prediction of the trajectory of the carbon–climate system at the same level of sophistication as a fully coupled carbon–climate model, it can provide information about the perturbation resulting from the presence or absence of a process P.

To illustrate this approach we have estimated the vulnerability of the carbon–climate system to one significant feedback, the carbon release from permafrost soils under the influence of warming (Zimov et al. 2006). Here, we assess the vulnerability due to CO_2 only (recognising that this is an underestimate of the true vulnerability because of the additional effect of CH_4) by using a simple, globally averaged 'box' carbon–climate model with the following attributes:

1. The model state vector includes six variables: mean global temperature (T_A), atmospheric CO_2 concentration ($[CO_2]_A$), the terrestrial carbon biomass excluding frozen soils (C_B), carbon store in permafrost or frozen soils (C_F), marine carbon store as dissolved inorganic carbon (C_M) and partial pressure of CO_2 in the upper ocean (pCO_2). Model equations and parameters are given in Tables 2.3–2.5.
2. Atmospheric CO_2 is connected to climate (T_A) through an overall climate sensitivity to CO_2 which parameterises not only the direct radiative forcing by CO_2 increases but also all other associated climate feedbacks (water vapour, clouds, …). Two alternative formulations are used, in which changes in T_A are proportional either to changes in $[CO_2]_A$ itself or to changes in $\ln [CO_2]_A$ (Table 2.3). The latter is consistent with classical radiative transfer theory for infrared absorption in

Raupach MR, Canadell JG (2008). Observing a vulnerable carbon cycle. In: The Continental-Scale Greenhouse Gas Balance of Europe (eds. AJ Dolman, R Valentini, A Freibauer). Springer, New York, p. 5-32.

Table 2.3 Governing equations for state variables in a simple box model of the carbon–climate system Carbon fluxes (F) are defined in Table 2.4; parameters are defined in Table 2.5

State variable		Governing equation
Mean global temperature (°C)	T_A	(1) Linear : $\frac{dT_A}{dt} = \alpha_1 \frac{d[CO_2]_A}{dt}$ (2) Logarithmic : $\frac{dT_A}{dt} = \frac{\alpha_2}{(\ln 2)[CO_2]_A} \frac{d[CO_2]_A}{dt}$
Atmospheric CO_2 concentration (ppm)	$[CO_2]_A$	$r_{CO_2} \frac{d[CO_2]_A}{dt} = F_{Foss} + F_{LUC} + F_{MA} + F_{FA} - \frac{dC_B}{dt}$
Terrestrial carbon store in biomass and soils (Pg C) excluding peatlands, frozen soils	C_B	$\frac{dC_B}{dt} = F_{NPP} - F_R - F_{LUC}$
Ocean (marine) carbon store (Pg C)	C_M	$\frac{dC_M}{dt} = -F_{MA}$
Ocean pCO_2 (Pa)	pCO_2	$\frac{dpCO_2}{dt} = \beta \frac{pCO_2}{C_M} \frac{dC_M}{dt}$
Carbon store in permafrost (frozen soils) (Pg C)	C_F	$\frac{dC_F}{dt} = -F_{FA}$

nearly saturated CO_2 bands (Arrhenius 1896; Goody 1964), while the former provides some account for positive feedbacks (e.g. from water vapour) which cause greenhouse warming to be greater than that for CO_2 alone. Each includes a single sensitivity parameter. Neither expression has a formal justification, but the differences between the two provide a first indication of the sensitivity of the carbon–climate system to assumptions about the CO_2–temperature coupling.

3. Frozen-soil carbon (C_F) is assumed to be released as CO_2 under the influence of global warming, from a pool initialised at a pre-industrial value $C_{F0} = 900$ Pg C (Zimov et al. 2006). The rate constant for this release (k_F) is zero in pre-industrial conditions ($T_A = T_{A0}$) and increases linearly with climate warming ($T_A - T_{A0}$) with a proportionality coefficient k_{FT}, so that $dC_F/dt = -k_{FT}(T_A - T_{A0})C_F$. To estimate k_{FT}, we use the estimate that a warming of 2 °C will lead to shrinking of the permafrost area by around 25% (Anisimov et al. 1999). Assuming that (1) this area decrease translates to a shrinkage of the C_F pool by the same factor and (2) the release occurs over 100 years, the implied value of k_{FT} is 0.25 per century per (2 °C) or 0.00125 °C^{-1} y^{-1}. A value of 0.001 °C^{-1} y^{-1} is used here. This is a conservative value, mainly because a warming of 2 °C is likely to occur over a shorter time than 100 years, which would increase the inferred value of k_{FT}.

Raupach MR, Canadell JG (2008). Observing a vulnerable carbon cycle. In: The Continental-Scale Greenhouse Gas Balance of Europe (eds. AJ Dolman, R Valentini, A Freibauer). Springer, New York, p. 5-32.

Table 2.4 Phenomenological equations for fluxes (F) in a simple box model of the carbon–climate system

Carbon flux (Pg C y^{-1})		Phenomenological equation
CO_2 emissions from fossil fuels and other industry	F_{Foss}	1751–2005: data (Marland et al. 2006) future to 2100: scenarios (Table 2.1)
Emissions from land-use change	F_{LUC}	1751–2005: data (Houghton, 1999, C2007) future to 2100: linear decline to zero in 2100
Terrestrial NPP	F_{NPP}	$F_{NPP} = F_{NPP0} + (F_{NPP2} - F_{NPP0})f$ $(C_A - C_{A0}, C_{A1} - C_{A0})$ with $f(x,a) = x^2/(x^2 + a^2)$, $C_A = r_{CO_2}[CO_2]_A$
Terrestrial respiration	F_R	$F_R = k_{B0} C_B 2^{(T_A - T_{A0})/\delta_{2T}}$
Ocean-air CO_2 flux	F_{MA}	$F_{MA} = \frac{\{A_{Ocean} v_{Piston}([pCO_2]_M - [pCO_2]_A)\}}{k_{Henry}}$
Permafrost-air CO_2 flux	F_{FA}	$F_{FA} = k_{FT}(T_A - T_{A0})C_F$
NPP net primary production		

Table 2.5 Parameters in a simple box model of the carbon–climate system

Parameter	Symbol	Value
Conversion for atmospheric CO_2 (ppm to Pg C)	r_{CO2}	2.181 Pg C ppm^{-1}
Linear climate sensitivity to C_A	α_1	0.008 °C ppm^{-1}
Logarithmic (CO_2 doubling) climate sensitivity to CO_2	α_2	2 °C
Revelle buffer factor for response of pCO_2 to C_M	B	12 (dimensionless)
Initial (pre-industrial) temperature	T_{A0}	15 °C
Initial (pre-industrial) CO_2 concentration	$[CO_2]_{A0}$	278 ppm
Initial (pre-industrial) terrestrial biomass C store	C_{B0}	Calculated (equilibrium)
Initial (pre-industrial) marine C store	C_{M0}	5,000 Pg C
Initial (pre-industrial) ocean pCO_2	$pCO_{2(0)}$	Calculated (equilibrium)
Initial (pre-industrial) C store in frozen soils	C_{F0}	500 Pg C
Initial (pre-industrial) NPP	F_{NPP0}	60 Pg C y^{-1}
NPP at saturation with respect to CO_2	F_{NPP2}	75 Pg C y^{-1}
CO_2 scale for NPP saturation with respect to CO_2	$[CO_2]_{A1}$	450 ppm
Turnover rate for terrestrial respiration at $T_A = T_{A0}$	k_{B0}	0.02 y^{-1}
Doubling temperature for F_R	δ_{2T}	15 °C
Ocean area	A_{Ocean}	3.6×10^{14} m^2
Ocean exchange (piston) velocity	v_{Piston}	1,500 m y^{-1}
Henry's law constant for CO_2	k_{Henry}	$2{,}900 \times 2^{[(25 - T_A)/25]}$ Pa m^3 mol^{-1}
Rate per °C for C flux from frozen soils	k_{FT}	0 or 0.001 y^{-1} $°C^{-1}$

NPP net primary production

Raupach MR, Canadell JG (2008). Observing a vulnerable carbon cycle. In: The Continental-Scale Greenhouse Gas Balance of Europe (eds. AJ Dolman, R Valentini, A Freibauer). Springer, New York, p. 5-32.

4. Parameters (particularly the climate sensitivities to CO_2) and initial conditions were chosen so that predictions approximately matched past (1750–2005) trends T_A and $[CO_2]_A$ (Table 2.5).

Figure 2.4 shows predictions for 1750–2100 under four IPCC SRES scenarios (Table 2.1), with no frozen-carbon feedback ($k_{FT} = 0$). Agreement with past observations of T_A and $[CO_2]_A$ is satisfactory. Predictions with a linear climate sensitivity to CO_2 (upper panels) yield a warming range in 2100 of 2 °C (scenario B1) to 4 °C (scenario A2), compared with 1.5–2.5 °C from the logarithmic climate sensitivity to CO_2. The former, larger warming is very close to the ensemble of climate model results in the IPCC Fourth Assessment Report (IPCC 2007), while the latter is lower. The $[CO_2]_A$ range is 560 ppm (scenario B1) to 820 ppm (scenario A2).

Figure 2.5 compares model predictions with the frozen-carbon pool disabled ($k_{FT} = 0$) and enabled ($k_{FT} = 0.001$ °C^{-1} y^{-1}), using future emissions scenario A2 (the standard scenario for C^{4}MIP). With linear climate sensitivity to CO_2 (which yields a model behaviour broadly consistent with IPCC predictions as noted above), the positive

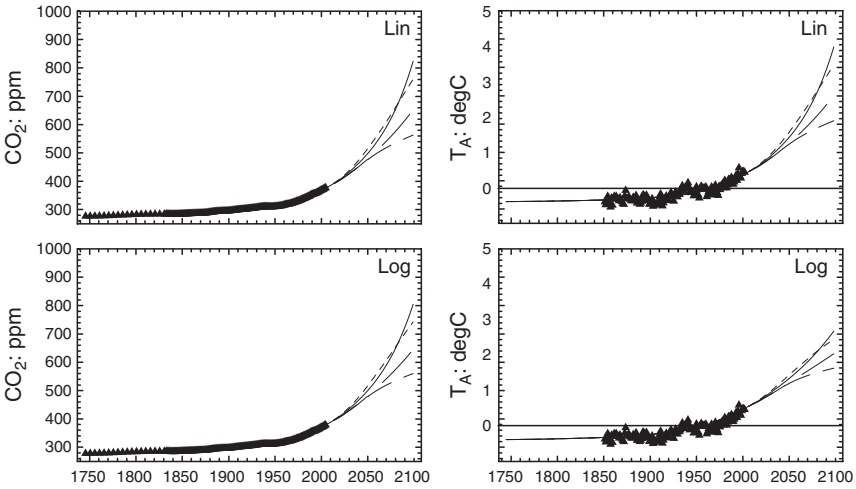

Fig. 2.4 Predictions from a simple box model of the carbon–climate system of atmospheric CO_2 concentration ($[CO_2]_A$, left panels) and global mean temperature (T_A, right panels). The zero line for T_A is set to the average observed T_A over the period 1961–1990. Four emissions scenarios are shown, comprising actual fossil-fuel and land-use-change emissions from 1751 to 2005 (data sources as in Fig. 2.1), and the A2 (solid), A1B (short dashed), B1 (medium dashed) and B2 (long dashed) scenarios (Nakicenovic et al. 2000) from 2005 to 2100. Upper and lower panels respectively show predictions with linear and logarithmic climate sensitivities to $[CO_2]_A$. Data (points) for $[CO_2]_A$ are composite observations from ice core data from Law Dome, Antarctica (Etheridge et al. 1998b) (before 1959) and direct atmospheric measurements at Mauna Loa, Hawaii (Keeling and Whorf 2005) (1959 onward). Data (points) for T_A are the global temperature series 1850–2004 (Jones et al. 2006).

Raupach MR, Canadell JG (2008). Observing a vulnerable carbon cycle. In: The Continental-Scale Greenhouse Gas Balance of Europe (eds. AJ Dolman, R Valentini, A Freibauer). Springer, New York, p. 5-32.

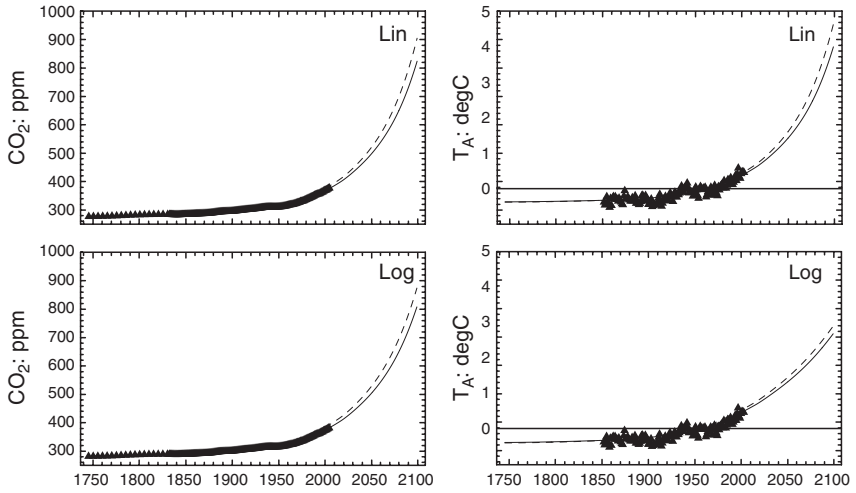

Fig. 2.5 Predictions from a simple box model of the carbon–climate system of atmospheric CO_2 concentration ($[CO_2]_A$, left panels) and global mean temperature (T_A, right panels) without (solid) and with (dashed) feedbacks between the frozen-carbon pool and global temperature. The emissions scenario comprises actual fossil-fuel and land-use-change emissions from 1751 to 2005 (data sources as in Fig. 2.1), and the A2 scenario from 2005 to 2100. Upper and lower panels respectively show predictions with linear and logarithmic climate sensitivities to $[CO_2]_A$. Data for $[CO_2]_A$ and T_A as in Fig. 2.4.

feedback on warming through CO_2 release from frozen soils yields an additional temperature increment in 2100 (δT_A) of about 0.7 °C and a CO_2 increment ($\delta[CO_2]_A$) of about 80 ppm, above the changes induced by other processes. The increments with the logarithmic climate sensitivity to CO_2 are lower, because vulnerability of frozen carbon increases with warming.

This simple calculation neglects the additional warming due to CH_4 release. From one estimate (Zimov et al. 2006), about 30% of the carbon released to the atmosphere from thawing permafrost is released as CH_4, with a present global warming potential (GWP) of about 21 relative to CO_2 (though the GWP of CH_4 will decline in the future). This methane has a residence time in the atmosphere of the order of 10 years, ultimately being oxidised to CO_2. Thus, the GWP of the released carbon decreases with time.

2.5 Implications of Carbon–Climate Vulnerabilities for Carbon Observation

Over several years, the global research and observation communities have been developing a concept for integrated global carbon observation. The carbon theme report of the Integrated Global Observing Strategy (Ciais et al. 2004) calls for integrated observations of fluxes, processes and pools, principally:

Raupach MR, Canadell JG (2008). Observing a vulnerable carbon cycle. In: The Continental-Scale Greenhouse Gas Balance of Europe (eds. AJ Dolman, R Valentini, A Freibauer). Springer, New York, p. 5-32.

- Satellite measurements of atmospheric-column CO_2, CH_4 and other GHGs, together with in situ (flask and continuous) measurements
- An operational, optimised network of eddy-covariance flux towers, measuring the CO_2 flux as NEE, with water and energy fluxes, over all major ecosystems
- A global system for in situ (ship, drifter) ocean pCO_2 measurements
- Satellite observations of vegetation and other land surface properties
- Georeferenced fossil-fuel emission maps including temporal variability and uncertainties
- Regular inventories of forest above-ground biomass and soil carbon content
- Regular inventories of dissolved carbon and related biogeochemical quantities in the ocean
- Satellite and in situ observations of fire, land cover change and other disturbance processes
- Monitoring of land-to-ocean carbon fluxes in river run off
- Monitoring of carbon fluxes associated with goods (harvesting, trade, disposal)

Many of these measurements (particularly the atmospheric concentrations and ocean biogeochemistry) are to be integrated with near-real-time modelling frameworks, using data assimilation into climate and earth system models. This may involve collaboration with the atmosphere–ocean models run by operational weather forecasting agencies, together with longer timescale models of pool dynamics in the carbon–climate system.

In Introduction, we highlighted two broad goals for a global carbon observing system, oriented respectively towards understanding and management. Recognition of carbon–climate vulnerabilities gives added focus to both goals, through the need to provide early warning of feedbacks (both positive and negative), to understand the reasons for emerging trends, and to provide national and international policy communities with information to manage vulnerabilities. Considering the carbon–climate vulnerabilities associated with terrestrial processes (Sect. 2.3 and Table 2.2), we now analyse the modes of terrestrial observation which emerge as having particular importance. Some are already well covered by existing plans, others less so. The discussion is organised around (1) fluxes and processes and (2) pools.

2.5.1 Fluxes and Processes

Additional observations are needed to increase our capacity to attribute carbon fluxes to specific source and sink processes, and to detect changes in the statistical properties of vulnerabilities associated with episodic disturbances. The following are key areas:

- *Responses of NPP and respiration to extreme events*: NPP and respiration respond not only to long-term climate shifts but also to extreme events (sometimes through threshold-like transitions), as has already been observed (Sect. 2.3.1). Observational requirements to improve detection and understanding of these effects include:

Raupach MR, Canadell JG (2008). Observing a vulnerable carbon cycle. In: The Continental-Scale Greenhouse Gas Balance of Europe (eds. AJ Dolman, R Valentini, A Freibauer). Springer, New York, p. 5-32.

- *Satellite measurements of vegetation dynamics over multi-year periods:* Longevity of satellite records requires rehabilitation and harmonisation of data from old systems with records extending back to the 1980s (e.g. AVHRR), together with maintenance of modern systems (e.g. MODIS) and launching of well-equipped new systems on the timescales required to maintain continuity through overlap between systems.
- *Process-based observations:* Flux towers and other process observations have a major role in the detection and attribution of the effects of drought and heat stress on production. Consistent long-term observations are critical for this purpose, to enable the extreme-event signal to emerge from the climatological background.

- *Multi-factorial of responses of NPP and respiration to temperature, water, nutrients and CO_2*: Climate-induced changes in the relationship between NPP and soil respiration have major implications for the terrestrial carbon balance, including NEE and pool dynamics. There is a wide scatter in existing process-based information on the responses of NPP, respiration and NEE to interactions among the drivers of temperature, water, nutrients and CO_2 (C2007; also see Sect. 2.3.1). It is important to attribute and hence reduce this scatter, which implies a continuing demand for ecosystem eddy flux measurements coupled with chamber-based soil measurements over diverse ecosystems (boreal, tundra, tropical, permafrost, temperate forests, semi-arid regions, etc.), together with ongoing multi-factorial manipulative experiments to disentangle the interactions.

- *Deforestation*: Carbon fluxes from deforestation remain the single most important direct human forcing of the terrestrial carbon balance, and the component of the global carbon budget with the largest uncertainty. To reduce this uncertainty, we need
  - Improved measurements of deforestation rates (including selective logging) from remote sensing
  - Improved biomass densities to calculate carbon emission factors
  - Improved knowledge of the time courses of carbon fluxes following deforestation (e.g. biomass cleared in 1 year may be burned in following years, and there are time lags associated with soil respiration). Yearly measurements deforestation would also help to attribute annual fluctuations in atmospheric CO_2 growth (current deforestation data is available only in increments of 5–10 years)

- *Fire*: This is another key process responsible for a large part of the perturbations in the annual CO_2 growth. Global improvement in estimates of both burned area and carbon emissions from fire will need to rely on atmospheric networks and remote sensing products. These observations include increased focus on (1) use of CO and CH_4 to quantify the contribution of fires to the atmospheric CO_2 growth (Langenfelds et al. 2002), (2) extraction of burned area (monthly) and hot spots (daily) from remote sensing, (3) ground and remote sensing observations of vegetation recovery after fire (when not linked to deforestation).

Raupach MR, Canadell JG (2008). Observing a vulnerable carbon cycle. In: The Continental-Scale Greenhouse Gas Balance of Europe (eds. AJ Dolman, R Valentini, A Freibauer). Springer, New York, p. 5-32.

2.5.2 Pools

In addition to existing and currently planned inventory networks for monitoring terrestrial carbon pools, two kinds of observations emerge as critical from a vulnerability standpoint:

- *Carbon in frozen soils*: Section 2.4 has offered a semi-quantitative analysis of the significant carbon–climate vulnerability associated with carbon stored in frozen soils at high northern latitudes, which are susceptible to decomposition under global warming. To improve estimates such as this one, it is important to monitor thawing trends and the resulting carbon emission, particularly its distribution between CO_2 and CH_4. Key measurements are:
  - Monitoring of the permafrost southern limit and changes in depth of permafrost
  - Carbon content in frozen soils, to full profile depth (substantially deeper than 1 m)
  - Measurements of vertical fluxes of CO_2 and CH_4 with eddy-covariance (local) and atmospheric-inverse (large regional) methods
  - Measurement of lateral carbon fluxes to rivers and the coastal zone
- *Peatlands*: Both in high latitudes (as a continuum of permafrost) and in the tropics, peatlands require careful monitoring of changes in stocks and fluxes under the influences of warming and changes in the hydrological cycle. Particularly in the tropics, changes in hydrological regime result both from climate change and from human activities such as drainage. Key measurements (similar to those for frozen soils) include:
  - Monitoring of tropical peatland deforestation and drainage
  - Carbon content to full profile depth (substantially deeper than 1 m)
  - Monitoring of vertical and lateral fluxes in both cold and tropical peatlands
  - Monitoring of subsidence rates of drained peatland forests

2.6 Conclusion

In Sect. 2.3, we identified several major carbon–climate vulnerabilities: limitation of CO_2 fertilisation by water and nutrient constraints, the response of soil respiration and NPP to warming and moisture, permafrost thawing, fire and ecosystem responses to a variety of land-use changes. A semi-quantitative assessment in Sect. 2.4 of just one of these vulnerabilities (the CO_2 consequence of permafrost thawing) suggests a perturbation on global CO_2 in 2100 of about 80 ppm and a temperature perturbation of about 0.7 °C, relative to a prediction under the A2 emissions scenario in which this positive feedback is absent. The temperature perturbation is a conservative estimate because of the neglect of warming due to CH_4. It is reasonable

Raupach MR, Canadell JG (2008). Observing a vulnerable carbon cycle. In: The Continental-Scale Greenhouse Gas Balance of Europe (eds. AJ Dolman, R Valentini, A Freibauer). Springer, New York, p. 5-32.

to conclude that the sum of all the vulnerabilities discussed in Sect. 2.3 is not negligible relative to the primary forcing of the climate system by anthropogenic CO_2. The implication for carbon observation is to focus attention on the process measurements and monitoring programmes needed to track and better quantify the feedback processes leading to these vulnerabilities.

Acknowledgements The work described here is a contribution to Theme 2 (Processes and Interactions) of the Global Carbon Project (www.globalcarbonproject.org). We are grateful to Cathy Trudinger and Will Steffen for constructive comments on drafts of this work, and Peter Briggs for assistance with figures. MRR thanks the CarboEurope Integrated Program for support to attend the CarboEurope Greenhouse Gas Workshop, Amsterdam, 4–5 April 2005, which prompted the writing of this chapter. We thank the Australian Greenhouse Office and CSIRO for supporting the GCP International Project Office in Canberra.

References

Achard F., Eva H. D., Mayaux P., Stibig H. J., Belward A. 2004. Improved estimates of net carbon emissions from land cover change in the tropics for the 1990s. Global Biogeochem. Cycles **18**: doi:10.1029/2003GB002142.

Allan W., Lowe D. C., Gomez A. J. 2005. Interannual variations of ^{13}C in tropospheric methane: Implication for a possible atomic chlorine sink in the marine boundary layer. J. Geophys. Res. **110**: doi:10.1029/ 2004JD005650.

Angert A., Biraud S., Bonfils C. et al. 2005. Drier summers cancel out the CO_2 uptake enhancement induced by warmer springs. Proc. Natl. Acad. Sci. U.S.A. **102**: 10823–10827.

Anisimov O. A., Nelson F. E., Pavlov A. V. 1999. Predictive scenarios of permafrost development under conditions of global climate change in the XXI century. Earth Cryol. **3**: 15–25.

Arrhenius S. 1896. On the influence of carbonic acid in the air upon the temperature of the ground. Philos. Mag. J. Sci. **5**: 239–276.

Bogner J., Matthews E. 2003. Global methane emissions from landfills: New methodology and annual estimates 1980–1996. Global Biogeochem. Cycles **17**: doi:10.1029/2002GB001913.

Bousquet P., Ciais P., Miller J. B. et al. 2006. Contribution of anthropogenic and natural sources to atmospheric methane variability. Nature **443**: 439–443.

Burrows W. H., Henry B. K., Back P. V. et al. 2002. Growth and carbon stock change in eucalypt woodlands in northeast Australia: Ecological and greenhouse sink implications. Global Change Biol. **8**: 769–784.

Camill P. 2005. Permafrost thaw accelerates in boreal peatlands during late-20th century climate warming. Clim. Change **68**: 135–152.

Canadell J. G., Le Quéré C., Raupach M. R., Field C. B., Buitenhuis E. T., Ciais P, Conway T. J., Gillette N. P., Houghton R. A., Marland G. 2007a. Contributions to accelerating atmospheric CO_2 growth from economic activity, carbon intensity, and efficiency of natural sinks. Proceedings of the National Academy of Sciences, Early Edition 10.1073/pnas.0702737104.

Canadell J. G., Pataki D., Gifford R. M. et al. 2007b. Saturation of the terrestrial carbon sink. In Terrestrial Ecosystems in a Changing World, eds. J. G. Canadell, D. Pataki, L. Pitelka, pp. 59–78. Springer-Verlag, Berlin.

Cao M. K., Gregson K., Marshall S. 1998. Global methane emission from wetlands and its sensitivity to climate change. Atmos. Environ. **32**: 3293–3299.

Chen Y.-H., Prinn R. G. 2005. Atmospheric modeling of high- and low-frequency methane observations: Importance of interannually varying transport. J. Geophys. Res. **110**: D10303, doi:10.1029/ 2004JD005542.

Raupach MR, Canadell JG (2008). Observing a vulnerable carbon cycle. In: The Continental-Scale Greenhouse Gas Balance of Europe (eds. AJ Dolman, R Valentini, A Freibauer). Springer, New York, p. 5-32.

Christiansen T. R., Ekberg A., Ström L., Mastepanov M. 2003. Factors controlling large scale variations in methane emission from wetlands. Geophys. Res. Lett. **30**: doi: 10.1029/ 2002GL016848.

Ciais P., Moore B. I., Steffen W. et al. 2004. *Integrated global carbon observation theme: A strategy to realise a coordinated system of integrated global carbon cycle observations*. Integrated Global Observing Strategy, Stockholm.

Ciais P., Reichstein M., Viovy N. et al. 2005. Europe-wide reduction in primary productivity caused by the heat and drought in 2003. Nature **437**: 529–533.

Cramer W., Bondeau A., Woodward F. I. et al. 2001. Global response of terrestrial ecosystem structure and function to CO_2 and climate change: Results from six dynamic global vegetation models. Global Change Biol. **7**: 357–373.

DeFries R. S., Field C. B., Fung I. Y., Collatz G. J., Bounoua L. 1999. Combining satellite data and biogeochemical models to estimate global effects of human-induced land cover change on carbon emissions and primary productivity. Global Biogeochem. Cycles **13**: 803–815.

DeFries R. S., Houghton R. A., Hansen M. C., Field C. B., Skole D., Townshend J. 2002. Carbon emissions from tropical deforestation and regrowth based on satellite observations for the 1980s and 1990s. Proc. Natl. Acad. Sci. U.S.A. **99**: 14256–14261.

Etheridge D. M., Steele L. P., Francey R. J., Langenfelds R. L. 1998a. Atmospheric methane between 1000 AD and present: Evidence of anthropogenic emissions and climatic variability. J. Geophys. Res. **103**: 15979–15993.

Etheridge D. M., Steele L. P., Langenfelds R. L., Francey R. J., Barnola J. M., Morgan V. I. 1998b. *Historical CO_2 records from the Law Dome DE08, DE08-2, and DSS ice cores*. Trends: A Compendium of Data on Global Change, Carbon Dioxide Information Analysis Center, Oak Ridge National Laboratory, U.S. Department of Energy, Oak Ridge, Tennessee, USA.

Fang J. Y., Chen A. P., Peng C. H., Zhao S. Q., Ci L. 2001. Changes in forest biomass carbon storage in China between 1949 and 1998. Science **292**: 2320–2322.

Fang C. M., Smith P., Moncrieff J. B., Smith J. U. 2005. Similar response of labile and resistant soil organic matter pools to changes in temperature. Nature **433**: 57–59.

Farquhar G. D., Sharkey T. D. 1982. Stomatal conductance and photosynthesis. Annu. Rev. Plant Physiol. **33**: 317–345.

Farquhar G. D., Caemmerer von S., Berry J. A. 1980. A biochemical model of photosynthetic CO_2 assimilation in leaves of C_3 species. Planta **149**: 78–90.

Field C. B., Raupach M. R. 2004. The Global Carbon Cycle: Integrating Humans, Climate, and the Natural World. Island Press, Washington, p. 526.

Field C. B., Chapin III F. S., Chiariello N. R., Holland E. A., Mooney H. A. 1996. The Jasper Ridge CO_2 experiment: Design and motivation. In Carbon Dioxide and Terrestrial Ecosystems, eds. G. W. Koch, H. A. Mooney, pp. 121–145. Academic Press, San Diego.

Friborg T., Soegaard H., Christensen T. R., Lloyd C. R., Panikov N. S. 2003. Siberian wetlands: Where a sink is a source. Geophys. Res. Lett. **30**.

Friedlingstein P., Cox P., Betts R. et al. 2006. Climate-carbon cycle feedback analysis: Results from the C4MIP model intercomparison. J. Clim. **19**: 3337–3353.

Fung I. Y., John J., Lerner J., Mathews E., Prather M., Steele L. P., Fraser P. J. 1991. Three-dimensional model synthesis of the global methane cycle. J. Geophys. Res. **96**: 13033–13065.

Giardina C. P., Ryan M. G. 2000. Biogeochemistry: Soil warming and organic carbon content - Reply. Nature **408**: 790.

Gifford R. M., Howden M. 2001. Vegetation thickening in an ecological perspective: Significance to national greenhouse gas inventories. Environ. Sci. Policy **4**: 59–72.

Global Carbon Project 2003. *Science Framework and Implementation*. Earth System Science Partnership (IGBP, IHDP, WCRP, Diversitas) Report No. 1; GCP Report No. 1, Global Carbon Project, Canberra.

Goody R. M. 1964. Atmospheric Radiation. I. Theoretical Basis. Clarendon Press, Oxford, 436 pp.

Greenblatt J. B., Sarmiento J. L. 2004. Variability and climate feedback mechanisms in ocean uptake of CO_2. In The Global Carbon Cycle: Integrating Humans, Climate, and the Natural World, eds. C. B. Field, M. R. Raupach, pp. 257–275. Island Press, Washington.

Raupach MR, Canadell JG (2008). Observing a vulnerable carbon cycle. In: The Continental-Scale Greenhouse Gas Balance of Europe (eds. AJ Dolman, R Valentini, A Freibauer). Springer, New York, p. 5-32.

Gruber N., Friedlingstein P., Field C. B. et al. 2004. The vulnerability of the carbon cycle in the 21st century: An assessment of carbon-climate-human interactions. In The Global Carbon Cycle: Integrating Humans, Climate, and the Natural World, eds. C. B. Field, M. R. Raupach, pp. 45–76. Island Press, Washington.

Hein R., Crutzen P. J., Heimann M. 1997. An inverse modelling approach to investigate the global atmospheric methane cycle. Global Biogeochem. Cycles **11**: 43–76.

Holland E. A., Braswell B. H., Lamarque J. F. et al. 1997. Variations in the predicted spatial distribution of atmospheric nitrogen deposition and their impact on carbon uptake by terrestrial ecosystems. J. Geophys. Res. Atmos. **102**: 15849–15866.

Houghton R. A. 1998. Historic role of forests in the global carbon cycle. In Carbon Dioxide Mitigation in Forestry and Wood Industry, eds. G. H. Kohlmaier, M. Weber, R. A. Houghton, pp. 1–24. Springer-Verlag, Berlin.

Houghton R. A. 1999. The annual net flux of carbon to the atmosphere from changes in land use 1850–1990. Tellus Ser. B **51**: 298–313.

Houghton R. A. 2003. Why are estimates of the terrestrial carbon balance so different? Global Change Biol. **9**: 500–509.

Houghton R. A., Hackler J. L. 2000. Changes in terrestrial carbon storage in the United States. 1: The roles of agriculture and forestry. Global Ecol. Biogeog. **9**: 125–144.

Houghton R. A., Hackler J. L., Lawrence K. T. 2000. Changes in terrestrial carbon storage in the United States. 2: The role of fire and fire management. Global Ecol. Biogeog. **9**: 145–170.

Houweling S., Kaminski T., Dentener F. J., Lelieveld J., Heimann M. 1999. Inverse modeling of methane sources and sinks using the adjoint of a global transport model. J. Geophys. Res. **104**: 26137–26160.

IPCC 2001. *Climate Change 2001: The Scientific Basis*. Contribution of Working Group I to the Third Assessment Report of the Intergovernmental Panel on Climate Change. Cambridge University Press, Cambridge, United Kingdom and New York.

IPCC 2007. *Climate change 2007: The physical science basis. Summary for policymakers*. IPCC Secretariat, Geneva.

Jacobson M., Charleson R. J., Rodhe H., Orians G. H. 2000. Earth System Science: From Biogeochemical Cycles to Global Change. Academic Press, New York, p. 527.

Janssens I. A., Freibauer A., Schlamadinger B. et al. 2005. The carbon budget of terrestrial ecosystems at country-scale - a European case study. Biogeosciences **2**: 15–26.

Jarvis P., Linder S. 2000. Botany: Constraints to growth of boreal forests. Nature **405**: 904–905.

Jones P. D., Parker D. E., Osborn T. J., Briffa K. R. 2006. *Global and hemispheric temperature anomalies - land and marine instrumental records*. Trends: A Compendium of Data on Global Change, Carbon Dioxide Information Analysis Center, Oak Ridge National Laboratory, U.S. Department of Energy, Oak Ridge, Tennessee, USA.

Jorgenson T. M., Shur Y. L., Pullman E. R. 2006. Abrupt increase in permafrost degradation in Arctic Alaska. Geophys. Res. Lett. **33**: doi:10. 1029/2005GL024960.

Keeling C. D. and Whorf T. P. 2005. *Atmospheric CO_2 records from sites in the SIO air sampling network*. Trends: A Compendium of Data on Global Change, Carbon Dioxide Information Analysis Center, Oak Ridge National Laboratory, U.S. Department of Energy, Oak Ridge, Tennessee, USA.

Knorr W., Prentice I. C., House J. I., Holland E. A. 2005. Long-term sensitivity of soil carbon turnover to warming. Nature **433**: 298–301.

Kurz W. A., Apps M. J. 1999. A 70-year retrospective analysis of carbon fluxes in the Canadian forest sector. Ecol. Appl. **9**: 526–547.

Langenfelds R. L., Francey R. J., Pak B. C., Steele L. P., Lloyd J., Trudinger C. M., Allison C. E. 2002. Interannual growth rate variations of atmospheric CO_2 and its delta C-13, H-2, CH_4, and CO between 1992 and 1999 linked to biomass burning. Global Biogeochem. Cycles **16**.

Le Quere C., Metzl N. 2004. Natural processes regulating the ocean uptake of CO_2. In The Global Carbon Cycle: Integrating Humans, Climate, and the Natural World, eds. C. B. Field, M. R. Raupach, pp. 243–255. Island Press, Washington.

Lelieveld J., Crutzen P. J., Dentener F. J. 1998. Changing concentration, lifetime and climate forcing of atmospheric methane. Tellus Ser. B **50**: 128–150.

Raupach MR, Canadell JG (2008). Observing a vulnerable carbon cycle. In: The Continental-Scale Greenhouse Gas Balance of Europe (eds. AJ Dolman, R Valentini, A Freibauer). Springer, New York, p. 5-32.

Lloyd J., Taylor J. A. 1994. On the temperature dependence of soil respiration. Functional Ecology **8**: 315–323.

Luger A. D., Moll E. J. 1993. Fire protection and afromontane forest expansion in Cape Fynbos. Biol. Conserv. **64**: 51–56.

Luo Y. Q., Wan S. Q., Hui D. F., Wallace L. L. 2001. Acclimatization of soil respiration to warming in a tall grass prairie. Nature **413**: 622–625.

Luo Y., Su B., Currie W. S. et al. 2004. Progressive nitrogen limitation of ecosystem responses to rising atmospheric carbon dioxide. BioScience **54**: 731–739.

Mack F., Hoffstadt J., Esser G., Goldammer J. G. 1996. Modeling the influence of vegetation fires on the global carbon cycle. In Biomass Burning and Global Change, ed. J. S. Levine. MIT Press, Cambridge, MA.

Marland G., Boden T. A., Andres R. J. 2006. *Global, regional, and national CO_2 emissions*. Trends: A Compendium of Data on Global Change, Carbon Dioxide Information Analysis Center, Oak Ridge National Laboratory, U.S. Department of Energy, Oak Ridge, Tennessee, USA.

Mikaloff Fletcher S. E., Tans P. P., Bruhwiler L. M., Miller J. B., Heimann M. 2004a. CH_4 sources estimated from atmospheric observations of CH_4 and its $^{13}C/^{12}C$ isotopic ratios: 1. Inverse modelling of source processes. Global Biogeochem. Cycles **18**: doi:10.1029/2004GB002223.

Mikaloff Fletcher S. E., Tans P. P., Bruhwiler L. M., Miller J. B., Heimann M. 2004b. CH_4 sources estimated from atmospheric observations of CH_4 and its $^{13}C/^{12}C$ isotopic ratios: 2. Inverse modelling of CH_4 fluxes from geographical regions. Global Biogeochem. Cycles **18**: doi:10.1029/2004GB002224.

Mosier A. R., Duxbury J. M., Freney J. R., Heinemeyer O., Minami K., Johnson D. E. 1998. Mitigating agricultural emissions of methane. Clim. Change **40**: 39–80.

Mouillot F., Field C. B. 2005. Fire history and the global carbon budget: A 1 degrees x 1 degrees fire history reconstruction for the 20th century. Global Change Biol. **11**: 398–420.

Nadelhoffer K. J., Emmett B. A., Gundersen P. et al. 1999. Nitrogen deposition makes a minor contribution to carbon sequestration in temperate forests. Nature **398**: 145–148.

Nakicenovic N., Alcamo J., Davis G. et al. 2000. *IPCC Special Report on Emissions Scenarios*. Cambridge University Press, Cambridge, U.K. and New York.

Nemani R. R., Keeling C. D., Hashimoto H. et al. 2003. Climate-driven increases in global terrestrial net primary production from 1982 to 1999. Science **300**: 1560–1563.

Norby R. J., DeLucia E. H., Gielen B. et al. 2005. Forest response to elevated CO_2 is conserved across a broad range of productivity. Proc. Natl. Acad. Sci. U.S.A. **102**: 18052–18056.

Nowak R. S., Ellsworth D. S., Smith S. D. 2004. Functional responses of plants to elevated atmospheric CO_2: Do photosynthetic and productivity data from FACE experiments support early predictions? New Phytol. **162**: 253–280.

Olivier J. G. J., Bouwman A. F., Berdowski J. J. M. et al. 1999. Sectoral emission inventories of greenhouse gases for 1990 on a per country basis as well as on 1x1. Environ. Sci. Policy **2**: 241–263.

Oren R., Ellsworth D. S., Johnsen K. H. et al. 2001. Soil fertility limits carbon sequestration by forest ecosystems in a CO_2-enriched atmosphere. Nature **411**: 469–472.

Owensby C. E., Ham J. M., Knapp A. K., Bremer D., Auen L. M. 1997. Water vapour fluxes and their impact under elevated CO_2 in a C4-tallgrass prairie. Global Change Biol. **3**: 189–195.

Pacala S. W., Hurtt G. C., Baker D. et al. 2001. Consistent land- and atmosphere-based US carbon sink estimates. Science **292**: 2316–2320.

Page S. E., Siegert F., Rieley J. O., Boehm H. D. V., Jaya A., Limin S. 2002. The amount of carbon released from peat and forest fires in Indonesia during 1997. Nature **420**: 61–65.

Page S. E., Wust R. A. J., Weiss D., Rieley J. O., Shotyk W., Limin S. H. 2004. A record of Late Pleistocene and Holocene carbon accumulation and climate change from an equatorial peat bog (Kalimantan, Indonesia): Implications for past, present and future carbon dynamics. J. Quat. Sci. **19**: 625–635.

Pataki D. E., Huxman T. E., Jordan D. N. et al. 2000. Water use of two Mojave Desert shrubs under elevated CO_2. Global Change Biol. **6**: 889–897.

Raupach MR, Canadell JG (2008). Observing a vulnerable carbon cycle. In: The Continental-Scale Greenhouse Gas Balance of Europe (eds. AJ Dolman, R Valentini, A Freibauer). Springer, New York, p. 5-32.

Raupach M. R., Marland G., Ciais P., LeQuere C., Canadell J. G., Field C. B. 2007. Global and regional drivers of accelerating CO_2 emissions. Proceedings of the National Academy of Sciences **14**: 10288–10293.

Raupach M. R., Rayner P. J., Barrett D. J. et al. 2005. Model-data synthesis in terrestrial carbon observation: Methods, data requirements and data uncertainty specifications. Global Change Biol. **11**: 10.1111/j.1365–2486.2005.00917.x.

Sabine C. L., Heimann M., Artaxo P. et al. 2004. Current status and past trends of the global carbon cycle. In The Global Carbon Cycle: Integrating Humans, Climate, and the Natural World, eds. C. B. Field, M. R. Raupach, pp. 17–44. Island Press, Washington.

Schellnhuber H. J., Cramer W., Nakicenovic N., Wigley T. M. L., Yohe G. 2006. Avoiding Dangerous Climate Change. Cambridge University Press, Cambridge, 392 pp.

Smith L. C., Sheng Y., MacDonald G. M., Hinzman L. D. 2005. Disappearing Arctic lakes. Science **308**: 1429.

Steffen W. L., Sanderson A., Tyson P. D. et al. 2004. Global Change and the Earth System: A Planet Under Pressure. Springer, Berlin, 336 pp.

Tarnocai C. 1999. The effect of climate warming on the carbon balance of cryosols in Canada. Permafrost Periglac. **10**: 251–263.

Townsend A. R., Braswell B. H., Holland E. A., Penner J. E. 1996. Spatial and temporal patterns in terrestrial carbon storage due to deposition of fossil fuel nitrogen. Ecol. Appl. **6**: 806–814.

Valentini R., Matteucci G., Dolman A. J. et al. 2000. Respiration as the main determinant of carbon balance in European forests. Nature **404**: 861–865.

van der Werf G. R., Randerson J. T., Collatz G. J., Giglio L. 2003. Carbon emissions from fires in tropical and subtropical ecosystems. Global Change Biol. **9**: 547–562.

van der Werf G. R., Randerson J. T., Collatz G. J. et al. 2004. Continental-scale partitioning of fire emissions during the 1997 to 2001 El Nino/La Nina period. Science **303**: 73–76.

van der Werf G. R., Randerson J. T., Giglio L., Collatz G. J., Kasibhatla P. S., Arellano A. F. 2006. Interannual variability in global biomass burning emissions from 1997 to 2004. Atmos. Chem. Phys. **6**: 3423–3441.

Wang J. S., Logan J. A., McElroy M. B., Duncan B. N., Megretskaia I. A., Yantosca R. M. 2004. A 3-D model analysis of the slowdown and interannual variability in the methane growth rate from 1988 to 1997. Global Biogeochem. Cycles **18**: GB3011, doi:10.1029/2003GB002180.

Wuebbles D. J., Hayhoe K. 2002. Atmospheric methane and global change. Earth-Sci. Rev. **57**: 177–210.

Zimov S. A., Schuur E. A. G., Chapin F. S. 2006. Permafrost and the global carbon budget. Science **312**: 1612–1613.

Raupach MR, Canadell JG (2008). Observing a vulnerable carbon cycle. In: The Continental-Scale Greenhouse Gas Balance of Europe (eds. AJ Dolman, R Valentini, A Freibauer). Springer, New York, p. 5-32.